Combined kinetic analysis for crystallization kinetics of non-crystalline solids

ARTICLE *in* JOURNAL OF NON-CRYSTALLINE SOLIDS · JUNE 2003

Impact Factor: 1.77 · DOI: 10.1016/S0022-3093(03)00023-1

3 AUTHORS:

Luis A Pérez-Maqueda
Spanish National Research Council
148 PUBLICATIONS **3,725** CITATIONS
SEE PROFILE

José M. Criado
Spanish National Research Council
242 PUBLICATIONS **5,663** CITATIONS
SEE PROFILE

Jiří Málek
University of Pardubice
218 PUBLICATIONS **4,143** CITATIONS
SEE PROFILE

Available online at www.sciencedirect.com
SCIENCE DIRECT®
Journal of Non-Crystalline Solids 320 (2003) 84–91
JOURNAL OF NON-CRYSTALLINE SOLIDS
www.elsevier.com/locate/jnoncrysol

Combined kinetic analysis for crystallization kinetics of non-crystalline solids

L.A. Pérez-Maqueda [a,*], J.M. Criado [a], J. Málek [b]

[a] CSIC-UNSE, Instituto de Ciencia de Materiales de Sevilla, Avd. Americo Vespucio s/n, Isla de la Cartuja, Sevilla 41010/41092, Spain
[b] Joint Laboratory of Solid State Chemistry, Studentská 84, 532 10 Pardubice, Czech Republic

Received 22 February 2002; received in revised form 5 November 2002

Abstract

A new method of kinetic analysis that allows the combined analysis of data obtained under different experimental conditions, i.e. heating pathway, is presented for the crystallization of non-crystalline solids. The method consists of a two-stage procedure. Firstly, an optimization procedure is applied for the determination of the Johnson, Mehl and Avrami (JMA). This optimization procedure is based on the linearization of the rate equation throw a logarithmic transformation; where the correlation coefficient function is the objective function, and the JMA order is the adjustable parameter. The JMA order obtained from this optimization procedure allows one to determine in a second stage the other kinetic parameters, i.e. activation energy and pre-exponential Arrhenius factor. The method proposed here allows one to analyze in a combined way data obtained under any heating profile, because no assumptions are made on the heating profile for the derivation of the rate equation. The method is tested with computed and experimental curves obtained under different heating conditions. The crystallization kinetics of $(GeS_2)_{0.3}(Sb_2S_3)_{0.7}$ glass are studied from the combined analysis of several curves.

1. Introduction

The crystallization kinetics of non-crystalline solids are extensively studied by thermal analysis methods such as differential thermal analysis (DTA), differential scanning calorimetry (DSC), or hot-stage X-ray diffraction. Experimental data are usually analyzed by means of the nucleation and growth model proposed by Johnson et al. [1–4] as shown by Christian [5]. The relationship between the reaction rate, $d\alpha/dt$, and the reacted fraction, α, at the time t, according to the Johnson, Mehl and Avrami (JMA) model, is given by the following expression:

$$\frac{d\alpha}{dt} = kn(1-\alpha)[-\ln(1-\alpha)]^{1-1/n}, \quad (1)$$

where n is a parameter that depends on the nucleation and growth mechanism and dimensionality and k is a rate constant that depends on the mechanisms of formation and growing of nuclei and is related with the temperature through the Arrhenius equation

* Corresponding author. Tel.: +34-954 489 532; fax: +34-954 460 565.
E-mail address: maqueda@cica.es (L.A. Pérez-Maqueda).

0022-3093/03/$ - see front matter © 2003 Elsevier Science B.V. All rights reserved.
doi:10.1016/S0022-3093(03)00023-1

$$k = A \cdot e^{-E/RT}, \quad (2)$$

where A is the pre-exponential factor of Arrhenius, E is the activation energy and T the absolute temperature. Table 1 includes the characteristic n parameters for different reaction mechanisms as taken from Ref. [6]. Eq. (1) should be fulfilled by reactions obeying the JMA kinetic law whatever would be the thermal pathway that has been followed for reaching a particular set of values $d\alpha/dt$–α–T [7]. However, it must be pointed out that the accomplishing of Eq. (1) all over the α range implies that k remains constant all over the process. Provided that the rate constant is depending on two processes: nucleation and growing of nuclei, the constancy of k would be expected only for reactions in which an instant nucleation followed by the growth of the formed nuclei occurs [8,9].

Experimental data for the kinetic analysis of crystallization of non-crystalline solids can be obtained under different temperature schedule. In the isothermal experiment, the sample is rapidly heated up to a temperature above glass transition and maintained at such temperature while the reaction evolution is recorded. Another alternative is the linear heating rate program where the reaction evolution is recorded during a single experiment in the whole range of temperatures. Several procedures have been proposed for determining the activation energy and the kinetic model from data obtained under rising temperature conditions [10–18]. Nevertheless, it has been pointed out [19–21] that both the activation energy and the kinetic model cannot be simultaneously obtained from a single experimental curve obtained under linear heating rate conditions. Following Maciejewsky and Vyazovkin's explanation [22], "this happens because in a single non-isothermal experiment both the temperature, T and extent of conversion, α vary simultaneously, and the approach generally fails to achieve separation of the reaction rate into the temperature dependence $k(T)$ and the reaction model $f(\alpha)$. As a result almost any $f(\alpha)$ can satisfactorily fit data at the cost of drastic variations in the Arrhenius parameters, which compensate for the difference between the assumed form of the $f(\alpha)$ and the true but unknown reaction model".

The aim of this paper is to present a general method for the combined kinetic analysis of crystallization data obtained under any experimental conditions, including the simultaneous kinetic analysis of a set of non-isothermal curves obtained at different heating rates. The method here

Table 1
Values of the exponent n for the JMA equation for different kinds of reaction mechanisms

Type of nucleation	Geometry of nuclei and their subsequent growth	Phase-boundary controlled	Diffusion controlled
Instantaneous nucleation (saturation of sites capable of nucleation prior to growth)	*Bulk mechanism*		
	One-dimensional growth	1	0.5
	Two-dimensional growth	2	1
	Three-dimensional growth	3	1.5
	Surface mechanism		
	Two-dimensional growth	~2	1
Constant rate of homogeneous nucleation during the process	*Bulk mechanism*		
	One-dimensional growth	2	1.5
	Two-dimensional growth	3	2
	Three-dimensional growth	4	2.5
	Surface mechanism		
	Two-dimensional growth	~3	~2
Decreasing nucleation rate (n_{dec})	$(n-1) < n_{dec} < n$		
Heterogeneous nucleation (n_{het})	$(n-1) < n_{het} < n$		
Increasing nucleation rate (n_{inc})	$n < n_{inc} < (n+1)$		

proposed is tested with calculated data and with experimental data for the crystallization kinetics of $(GeS_2)_{0.3}(Sb_2S_3)_{0.7}$ glass.

On the other hand, the application of the modulated-temperature heating program to the kinetics of crystallization of glasses will be considered. Modulated DSC, where a sinusoidal temperature modulation is superimposed on the underlying conventional heating profile [23–25], is a relatively new technique for distinguishing reversible and irreversible contributions to thermal transition of glasses, but it has still not been used for studying crystallization kinetics.

2. Computational procedure

2.1. Calculation of theoretical curves

Eqs. (1) and (2) can be rearranged in the form

$$\frac{d\alpha}{dt} = A\exp(-E/RT)n(1-\alpha)[-\ln(1-\alpha)]^{1-1/n}. \tag{3}$$

Eq. (3) will be used from here after for performing the kinetic analysis of computed and experimental $d\alpha/dt$–T (or t) plots. This equation is also used for calculating the theoretical curves representing $d\alpha/dt$ versus time or temperature. For isothermal conditions, temperature is maintained constant along the entire process, the term $A\exp(-E/RT)$ remains constant and Eq. (3) can be integrated in the following form:

$$(-\ln(1-\alpha))^{1/n} = A\exp(-E/RT)t. \tag{4}$$

The isothermal plot of $d\alpha/dt$ as a function of the time for given values of n, E and A can be calculated from Eqs. (3) and (4).

For the calculation of theoretical curves under linear heating rate conditions, Eq. (3) has been numerically integrated by means of the Runge–Kutta algorithm included in the Mathcad software [26] after considering the relationship between temperature and time through the heating rate ($\beta = dT/dt$); for the calculations, the converge tolerance was set in 10^{-5}%.

In the case of modulated-temperature programs, a sinusoidal temperature modulation is superimposed to the conventional temperature program, usually a linear heating one. Thus, the heating rate could be defined as follows:

$$\beta = \beta_0 + B\sin(\omega t), \tag{5}$$

where β_0 is the constant heating rate, B is the amplitude of the modulation and ω is the frequency. For the simulation of curves under this experimental conditions, the system of differential equations constituted by Eqs. (3) and (5) has been numerically solved by means of the same numerical procedure as described above for conventional linear heating rate conditions.

2.2. Kinetic analysis

After rearranging terms, Eq. (3) can be written in the following logarithmic form:

$$\ln\left(\frac{d\alpha/dt}{n(1-\alpha)[-\ln(1-\alpha)]^{1-1/n}}\right) = \ln A - E/RT. \tag{6}$$

The plot of the left-hand side of Eq. (6) versus the reciprocal of temperature yields a straight line if the correct n parameter is assumed. From this plot, the activation energy, E, is obtained from the slope, while the preexponential factor, A, is obtained from the intercept [10]. The method proposed here for determining the kinetic parameters consists in a two stages procedure. In a first stage, the Pearson's linear correlation coefficient for the left-hand side of Eq. (6) and the reciprocal of temperature is used as objective function for optimization. In this optimization process, n, is the variable parameter while the objective function is maximized. Optimization has been performed here by means of the *maximize* function of Mathcad software [26], any other optimization software can be used as, for example, the *Solver* macro included in Microsoft Excel. By this procedure, the parameter n that yields the best linear correlation for the plot of the left-hand side of Eq. (6) versus the reciprocal of temperature is obtained. This n parameter corresponds to the actual nucleation and growth mechanism and dimensionality. In a second stage, the so-obtained n parameter is substituted in Eq. (6) and from the plot of the left-hand

side of Eq. (6) versus the reciprocal of temperature the activation energy and the pre-exponential factors are determined from the slope and the intercept, respectively.

3. Experimental details

Sample of $(GeS_2)_{0.3}(Sb_2S_3)_{0.7}$ glass was prepared in a evacuated silica ampoule from pure elements (99.999% purity), by melting and homogenization at 950 °C for 12 h.

Differential scanning calorimetric (DSC) measurements were performed on ~10 mg bulk sample encapsulated in standard aluminum sample pans, in an atmosphere of dry nitrogen. The instrument was calibrated with indium, lead and zinc standards. Experiments were performed under linear heating rate conditions.

4. Results and discussion

4.1. Test of the method with simulated curves

The scope of this section is, firstly, to show that a single DSC trace recorded under a linear heating program can be exactly matched by assuming any value of n but leading to quite different activation energies depending on the n value previously assumed. Secondly, we will try to show that this misfortune (that it is not possible to determine the kinetic parameters of a crystallization reaction from a single DSC curve) is overcome by performing the simultaneous kinetic analysis of a set of DSC diagrams obtained under different thermal pathways. The use of calculated curves for this purpose would be convenient because they can be computed with a very large precision avoiding the uncertainty of experimental data.

Fig. 1 shows a theoretical curve generated for linear heating rate conditions (heating rate, $\beta = 10$ K min^{-1}), and the following kinetic parameters: $n = 2$, $E = 100$ kJ mol^{-1} and $A = 10^5$ min^{-1}. The computation was performed by numerical integration using the procedure reported above. This curve was analyzed by means of the conventional differential kinetic analysis method represented by

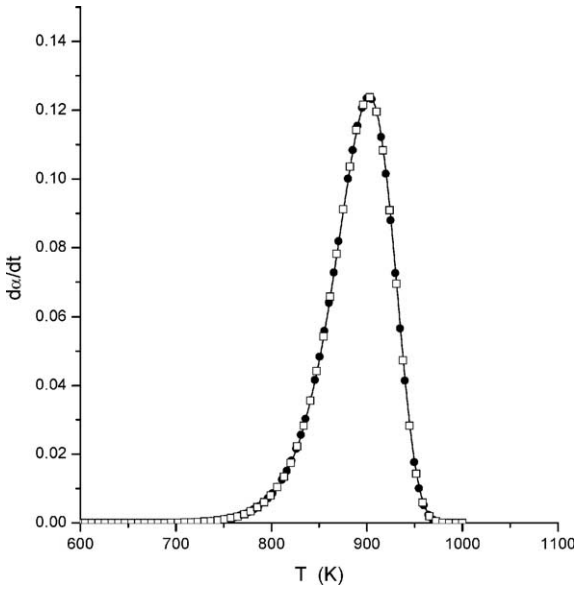

Fig. 1. Theoretical curves computed for linear heating rate conditions (heating rate, β, 10 K min^{-1}), and the following kinetic parameters: $n = 2$, $E = 100$ kJ mol^{-1} and $A = 10^5$ min^{-1} (solid line); $n = 2.5$, $E = 77.4$ kJ mol^{-1} and $A = 4 \times 10^4$ min^{-1} (□); $n = 3$, $E = 62.3$ kJ mol^{-1} and $A = 4.5 \times 10^2$ min^{-1} (●).

Eq. (6). Thus, the kinetic parameters were obtained from the plot of the left-hand side of Eq. (6) versus the inverse of temperature after assuming different values of n. Table 2 includes the activation energies and the preexponential factors of Arrhenius obtained from the simulated curve for different values of n. Table 2 shows that any n parameter yields a high correlation coefficient and, therefore, it is not possible to determine the n parameter and to obtain the kinetic parameters from

Table 2
Kinetic parameters (n, E) and correlation coefficient, r, obtained from the computed curve illustrated in Fig. 1 and analyzed by means of the differential kinetic analysis method represented by Eq. (8) for different n values

n	E (kJ mol^{-1})	A (min^{-1})	r
1.5	137.5	2×10^7	1.00000
2	100.0	10^5	1.00000
2.5	77.4	4×10^3	1.00000
3	63.4	4.5×10^2	1.00000
3.5	51.6	92	1.00000
4	43.6	28	1.00000

a single experimental DTA or DSC curve obtained under linear heating rate conditions [19,20]. In addition, it is also clear from Table 2 that kinetic parameters obtained from a single experimental curve are strongly dependent on the n coefficient previously assumed. Fig. 1 confirms the above conclusion; thus, this figure includes three DSC (or DTA) traces computed for linear heating rate conditions, $n = 2$, 2.5 and 3, and the kinetic parameters obtained from Table 2. It is clear from this figure (Fig. 1) that the three curves simulated assuming different kinetic parameters overlap completely, and it is not possible to differentiate among them from a single DSC (or DTA) trace. Nevertheless, when a set of different curves obtained under different heating rate conditions are analyzed simultaneously, only one kinetic model fits all the data and yields a single straight line. Fig. 2 includes a set of curves simulated under different linear heating rates, i.e. 5, 10 and 20 K min^{-1}, after assuming the kinetic parameters included in the figure caption. These data can be simultaneously analyzed by means of Eq. (6) because, as it was stated above, any set of $d\alpha/dt$–α–T experimental data obtained for the same solid state reaction under different heating profiles should fit this equation simultaneously. Fig. 3 shows the curves included in Fig. 2 analyzed simultaneously by means of Eq. (6) after assuming different n values. It is clear from this figure that only when the correct n parameter is assumed the data lie on a single straight line, otherwise, points are distributed in different parallel lines, one for each heating rate experiment. Data included in Fig. 2 were also analyzed by means of the optimization procedure described above. From the optimization procedure, the maximum Pearson's coefficient ($r = 1.00000$) was obtained for $n = 2$. After substituting this n parameter into Eq. (6), from the plot of the left-hand side of this equation versus the reciprocal of the temperature was obtained the activation energy and the preexponential factor of Arrhenius, $E = 100$ kJ mol^{-1} and $A = 10^5$ min^{-1}. This procedure yields the same kinetic parameters as those

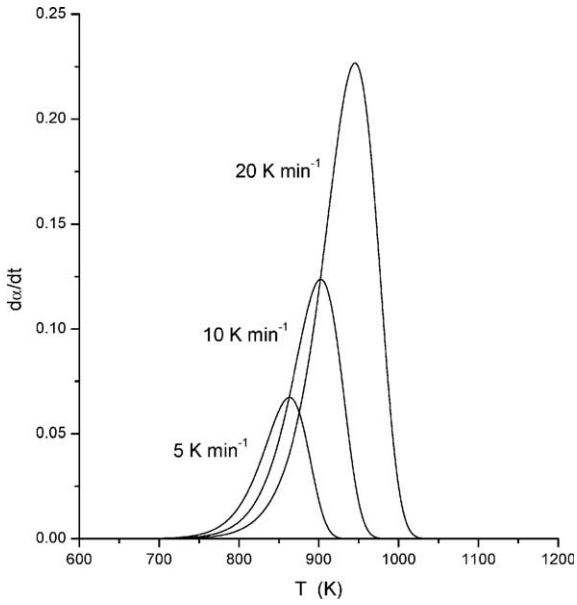

Fig. 2. Theoretical curves computed for linear heating rate conditions (5, 10 and 20 K min^{-1}) assuming the following kinetic parameters: $n = 2$, $E = 100$ kJ mol^{-1} and $A = 10^5$ min^{-1}.

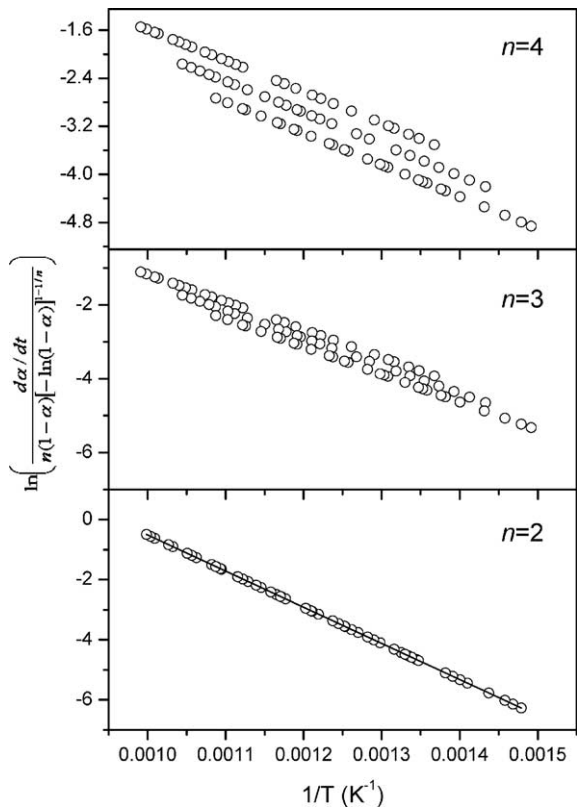

Fig. 3. Analysis of curves included in Fig. 2 by means of Eq. (8) for different n parameters.

used for the simulation confirming the validity of this analysis procedure.

As mentioned earlier Eq. (6) is a general equation and no assumptions are made on the way samples are heated; the procedure presented here is valid for any data obtained under any experimental conditions. In order to test the validity of the method for analyzing data obtained under different experimental conditions, a set of three curves (Fig. 4) has been simulated assuming in all cases an A3 ($n = 3$) kinetic model and the following kinetic parameters: $A = 10^4$ min^{-1}, $E = 80$ kJ mol^{-1}. One curve has been simulated assuming linear heating rate conditions (10 K min^{-1}), another curve has been constructed supposing isothermal conditions at $T = 800$ K and, finally, the last curve has been simulated assuming a modulated-temperature program where $\beta_0 = 1$ K min^{-1}, $B = 2$ K min^{-1}, and $\omega = 2$ min^{-1}. The optimization procedure yielded a maximum Pearson's coefficient ($r = 1.00000$) for $n = 3$. The plot of the left-hand side of Eq. (6) versus the reciprocal of temperature for the n coefficient ($n = 3$) obtained from the optimization procedure is shown in Fig. 5. All points are on a straight line as expected for a correlation coefficient of 1.00000. From this plot, it was obtained an activation energy $E = 80$ kJ mol^{-1} and a pre-exponential factor of Arrhenius $A = 10^4$ min^{-1} that were coincident with those assumed in the calculation with an error lower than 10^{-3}%. In summary, these results show that any set of α–dα/dt–T obtained under any experimental conditions could be analyzed by means of the procedure presented above yielding the correct kinetic parameters.

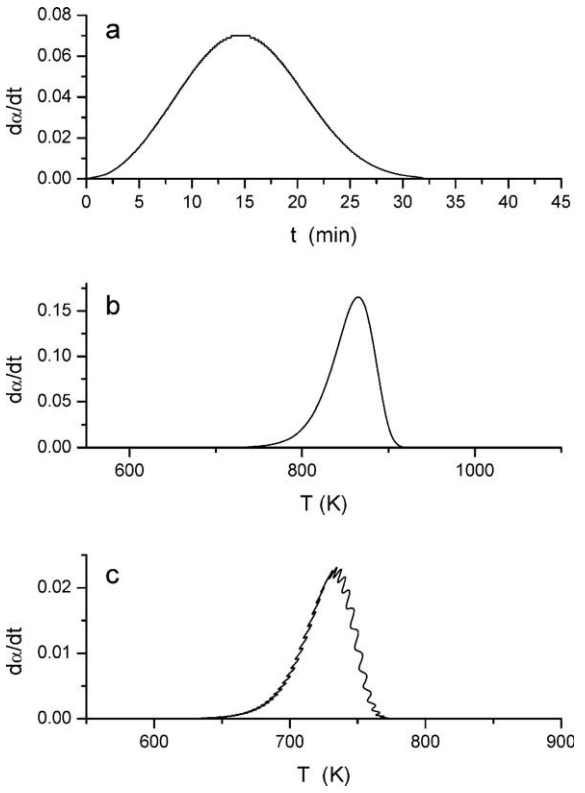

Fig. 4. Simulated curves under the following conditions: (a) isothermal conditions ($T = 800$ K); (b) linear heating rate conditions (10 K min^{-1}); (c) modulated-temperature program where $\beta_0 = 1$ K min^{-1}, $B = 2$ K, and $\omega = 2$ min^{-1}. In all cases $n = 3$, $A = 10^4$ min^{-1}, $E = 80$ kJ mol^{-1}.

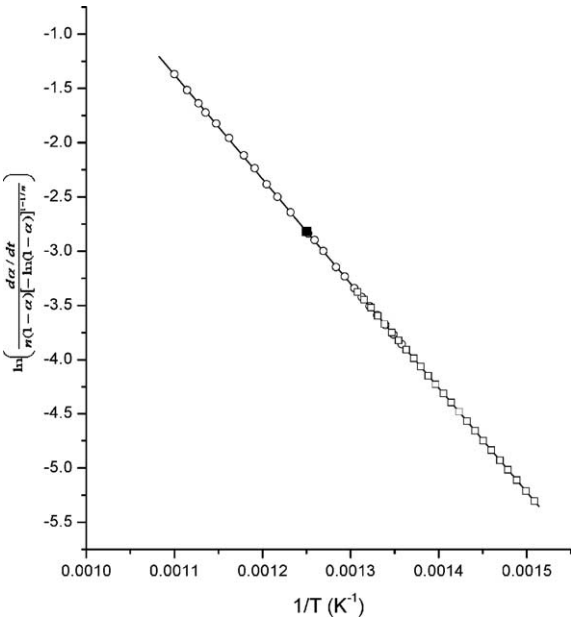

Fig. 5. Combined analysis of curves included in Fig. 4 by means of Eq. (8) for $n = 3$. (■) isothermal conditions, (○) linear heating rate conditions, and (□) modulated-temperature program.

4.2. Verification proposed with experimental data

Once it has been proved from theoretical data the validity of the method of kinetic analysis here

proposed it would be interesting to check its application using experimental data. A vast literature is available for the crystallization kinetics of oxide and chalcogenide glasses [27–32] but the raw experimental data obtained under different thermal pathways are not generally available from the papers to be reanalyzed by the method described in the previous section. The crystallization of the $(GeS_2)_{0.3}(Sb_2S_3)_{0.7}$ glass has been chosen because we have available samples of the same batch used in a previous paper [33] in which a detailed kinetic analysis was carried out from isoconversional methods.

Fig. 6 includes the DSC traces recorded at different heating rates, i.e. 2, 5, 10, 15 K min^{-1}, for the bulk crystallization of the $(GeS_2)_{0.3}(Sb_2S_3)_{0.7}$ glass. The combined kinetic analysis of these curves was performed by means of the procedure described above. Experimental data were analyzed in the range of α from 0.1 to 0.85 to avoid the deviations due to experimental errors for very high and low values of α. The optimization procedure yielded $n = 2.26$. The plot of the left-hand side of Eq. (6) versus the reciprocal of temperature for the obtained n coefficient yields a straight line (Fig. 7), whose slope and intercept leads, respectively, to an activation energy $E = 176 \pm 2$ kJ mol^{-1} and $A = (3.3 \pm 0.3)\ 10^{13}$ min^{-1}. These results are in agreement with those previously obtained by Málek [33] using the same batch sample and with those reported by Rysavá et al. [34] for a different sample preparation with the same composition. Finally, in order to test the validity of the calculated parameters, the experimental curves were reconstructed with these calculated parameters (Fig. 6). The good agreement between calculated and experimental curves for the four experiments proves the validity of the kinetic parameters calculated by this new kinetic method.

The combined analysis of the DSC curves recorded under different heating rates for the crystallization of $(GeS_2)_{0.3}(Sb_2S_3)_{0.7}$ glass allows one to conclude that the reaction rate of this process follows an Avrami–Erofeev mechanism with values of the activation energy and the pre-exponential factor of Arrhenius that remain constant all

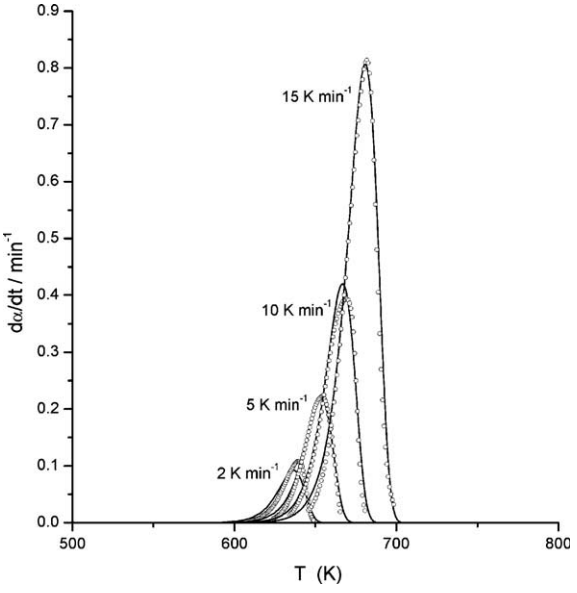

Fig. 6. DSC traces recorded at different heating rates, i.e. 2, 5, 10, 15 K min^{-1}, for the bulk crystallization of the $(GeS_2)_{0.3}(Sb_2S_3)_{0.7}$ glass (○). Reconstructed curves with the kinetic parameters obtained from the combined kinetic analysis of all the experimental curves, i.e. $n = 2.26$, $A = 3.3 \times 10^{13}$ min^{-1}, $E = 176$ kJ mol^{-1} (solid line).

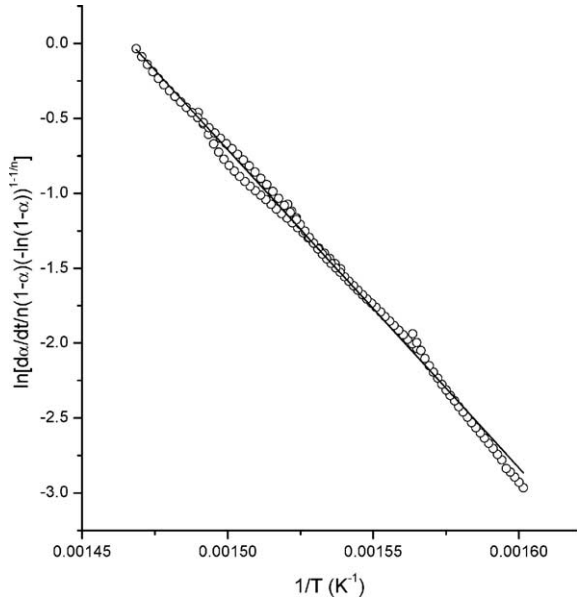

Fig. 7. Plot of the left-hand side of Eq. (8) versus the inverse of temperature for the optimum n coefficient ($n = 2.26$) for the experimental data represented in Fig. 6.

over the crystallization process. This behavior indicates that nucleation is completed in the sample before the growth process is started and, therefore, the crystallization rate of $(GeS_2)_{0.3}(Sb_2S_3)_{0.7}$ bulk glass is controlled by the growing of preexisting nuclei [35]. As mentioned above, under these conditions, the validity of the JMA kinetic model can be extended to non-isothermal conditions.

5. Conclusions

The following conclusions can be made from theoretical and experimental data:

1. A single $d\alpha/dt$–T plot obtained for a crystallization process obeying the JMA necessarily fits Eq. (3) whatever would be the value of the coefficient n previously assumed but leading to values of E quite different of the true one obtained by substituting the true value of n in Eq. (3). As a consequence the values of E, A and n cannot be simultaneously determined from a single DSC curve.
2. The combined analysis of a set of DSC plots obtained under different thermal pathways according with the method outlined in this paper permits one to determine without ambiguities the true kinetic parameters of crystallization reactions.

References

[1] W.A. Johnson, K.F. Mehl, Trans. Am. Inst. Min. (Metall.) Eng. 135 (1939) 416.
[2] M. Avrami, J. Chem. Phys. 7 (1939) 1103.
[3] M. Avrami, J. Chem. Phys. 8 (1940) 212.
[4] M. Avrami, J. Chem. Phys. 9 (1941) 177.
[5] J.W. Christian, Theory of Transformations in Metals and Alloys, 2nd Ed., Pergamon, New York, 1975.
[6] J. Sestak, in: G. Svehla (Ed.), Comprehensive Analytical Chemistry, vol. XII, Elsevier, Amsterdam, 1984, p. 191.
[7] L.A. Pérez-Maqueda, J.M. Criado, F.J. Gotor, J. Málek, J. Phys. Chem. A 106 (2002) 2862.
[8] D.W. Henderson, J. Therm. Anal. 15 (1979) 325.
[9] D.W. Henderson, J. Non-Cryst. Solids 30 (1979) 301.
[10] A.K. Galwey, M.E. Brown, in: M.E. Brown (Ed.), Handbook of Thermal Analysis and Calorimetry, Principles and Practise, vol. 1, Elsevier Science, Amsterdam, 1998, p. 147.
[11] J.H. Sharp, G.W. Brindley, B.N.N. Archar, J. Am. Ceram. Soc. 49 (1966) 379.
[12] M.E. Brown, D. Dolimore, A.K. Galwey, Thermochim. Acta 21 (1977) 103.
[13] M.E. Brown, D. Dolimore, A.K. Galwey, J. Chem. Soc. Faraday Trans. 70 (1974) 1316.
[14] E.S. Freeman, B. Carrol, J. Phys. Chem. 62 (1958) 394.
[15] H.L. Friedman, J. Polym. Sci. 66 (1965) 183.
[16] T. Ozawa, Bull. Chem. Soc. Jpn. 38 (1965) 1881.
[17] S. Vyazovkin, D. Dollimore, J. Chem. Inform. Comput. Sci. 36 (1996) 42.
[18] H.E. Kissinger, Anal. Chem. 29 (1957) 1702.
[19] J.M. Criado, J. Morales, Thermochim. Acta 19 (1977) 305.
[20] J.M. Criado, A. Ortega, J. Therm. Anal. 29 (1984) 1225.
[21] J. Málek, Thermochim. Acta 200 (1992) 257.
[22] M. Maciejewski, S. Vyazovkin, Thermochim. Acta 370 (2001) 149.
[23] M. Reading, Thermochim. Acta 292 (1997) 179.
[24] M. Reading, R. Luyt, J. Therm. Anal. Calorim. 54 (1998) 535.
[25] T. Ozawa, Thermochim. Acta 356 (2000) 173.
[26] Mathcad_2000_professional, MathSoft, Inc., 2000.
[27] S.A. Khan, M. Zulfequar, M. Husain, J. Phys. Chem. Solids 63 (2002) 1787.
[28] M.M.A. Imran, N.S. Saxena, Y.K. Vijay, R. Vijayvergiya, N.B. Maharjan, M. Husain, J. Non-Cryst. Solids 298 (2002) 53.
[29] L.A. Wahab, S.A. Fayek, A.H. Ashour, Mater. Chem. Phys. 68 (2001) 272.
[30] P. Rocabois, J.N. Pontoire, J. Lehmann, H. Gaye, J. Non-Cryst. Solids 282 (2001) 98.
[31] I. Shaltout, J. Mater. Sci. 35 (2000) 323.
[32] K.G. Cheng, J.L. Wan, K.M. Liang, J. Am. Ceram. Soc. 82 (1999) 1212.
[33] J. Málek, Thermochim. Acta 355 (2000) 239.
[34] N. Rysavá, C. Barta, L. Tichý, J. Mater. Sci. Lett. 8 (1989) 91.
[35] J. Málek, Thermochim. Acta 355 (2000) 239.